

Performances analysis of moving target tracking in circular SAR

Jean-Baptiste Poisson^{*}, H el ene Oriot^{*}, Florence Tupin^{**}

^{*}ONERA DEMR

Chemin de la Huni ere, 91761 Palaiseau Cedex, FRANCE

email: jean-baptiste.poisson@onera.fr

^{**}Institut T el ecom, T el ecom ParisTech

46 rue Barrault, F-75634 Paris Cedex 13, FRANCE

Abstract: *Ground moving target focusing and tracking using airborne data is a subject of increasing interest. Single antenna processing allows focusing [1] and azimuthal velocity estimation [2][3] under the assumption that the signal-to-clutter ratio (SCR) is high enough (for instance, 14dB in [3]), which is mostly not the case in an urban context. Moreover, these methods are insufficient to geolocalize the moving targets. Acquisition of SAR data over a circular path eliminate this drawback, because objects may be seen at a 360  angle and during a longer time than in the case of linear path. A technique to track moving targets in SAR images with only one sensor and using a circular path has been presented in [4]. In this paper, we perform a physical and geometrical analysis of this method and present accuracy evaluations. Finally some new results are presented on real data acquired around the city of N imes (X band).*

1. Introduction

Ground moving target focusing and tracking using airborne data is a subject of increasing interest. Because of target movements, a defocusing effect and delocalization in the azimuth direction may appear. Standard single antenna processing allows focusing [1] and velocity estimation [2][3] by taking advantage of these effects, but the SCR has to be high enough (14 dB in [3]), and in most cases in urban context, the SCR is lower than 14dB. Moreover, these methods are insufficient to geolocalize the moving targets. Acquisitions of SAR data over a circular path eliminate this drawback, because objects may be seen at a 360  angle. Moreover, the continuity of the SAR-platform movement may enhance moving target tracking. In a previous paper, having SAR images acquired along a circular trajectory in spotlight mode, we have presented an inversion method to retrieve the target position and velocity from the apparent coordinates of the moving targets in these SAR images and the estimated azimuthal velocity [4]. In this paper, we perform a physical and geometrical analysis of this method and present accuracy evaluation. In part one, we present the estimation of the covariance measurement matrix. Then, we estimate the covariance matrix of the output parameters given measurement accuracies, then we show some examples of the estimated position accuracy of synthetic target trajectories, and finally we show results obtained on real data around the city of Nimes.

2. Inversion method

In a previous paper [4], we have presented an inversion method to retrieve the target trajectory from the apparent coordinates of the moving targets in a set of SAR images acquired along a circular trajectory in spotlight mode. This method consisted in inverting a $3 \times N$ equation system, N being the number of images used to solve the problem, and each image gives 3 equations as follows:

$$\begin{cases} MP = D \\ \overrightarrow{MP} \cdot \vec{V} = D \cdot V \left(\sin(\theta_Q) - \frac{V_r}{V_s} \right) \\ \alpha = \frac{4\pi}{\lambda} \left(\frac{V^2}{2D} - \frac{V_s V_l}{D} + \frac{A_r}{2} \right) \end{cases}$$

V_l and V_r are the projection of the target velocity \vec{V} (with magnitude V) in the azimuth and range direction, and A_r the radial acceleration. V_s is the SAR platform velocity and D is the distance between the moving target P and the sensor M . α is the defocusing parameter, and θ_Q is the apparent squint angle of the moving target P (the real squint angle of a still target Q).

Two different hypotheses are used: first, we consider that targets have a constant acceleration during $N\Delta T$, where ΔT is the time interval between two images. Secondly, we consider that the target velocity and acceleration are collinear, so we look for targets moving along a straight line during calculation time.

For each image three measurements are needed: the two coordinates of the apparent position of the target and the defocusing parameter alpha. The focusing parameter alpha is retrieved from the measurements by fitting a parabola to the phase history of the target. [4]. Then, the target is refocused thanks to this parameter and the apparent position of the target is estimated (see Fig 1).

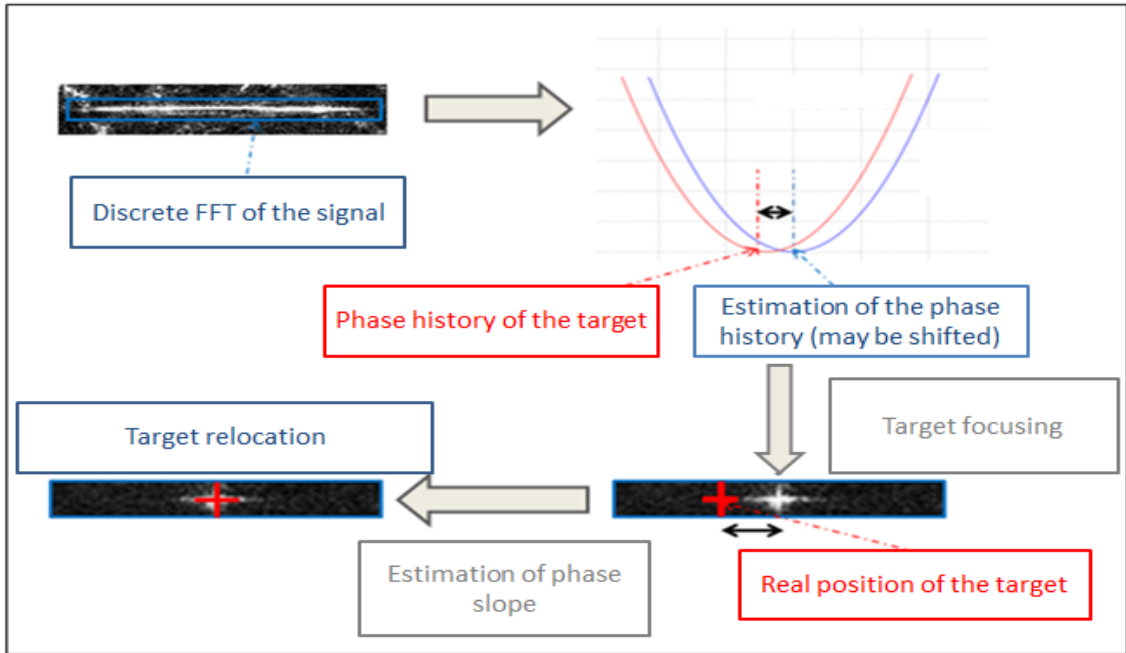


Fig. 1 : general overview of the measurement method

3. Estimation of the measurements accuracy

In order to estimate the accuracy of our inversion regarding the measurement accuracy, we use two different models. The first one is to consider targets as point-like scatterers, which is the ideal case, the second one considers extended targets.

3.1 Measurement accuracy: the point-like scatterers model:

With this target model, we consider that targets have no physical surfaces. So the target signal power only depends on the radar cross section (RCS) of the target:

$$P_{signal,dB} = RCS$$

The clutter power depends on the backscattering coefficient of the surface and on the resolution. The backscattering coefficient (σ^0) are given by Ulaby [6]. The clutter power is given by:

$$P_{clutter,dB} = \sigma^0 + 10\log(\rho_r * \rho_a)$$

Consequently, the signal to clutter ratio (SCR) which is given by $SCR = \frac{P_{signal}}{P_{clutter}}$ increases with the azimuth resolution. Ye et al. [7] give us the phase measurement accuracy in the case of a poinlike isotropic scatterer:

$$\sigma_\varphi = \frac{1}{\sqrt{2SCR}}$$

The estimation of the phase history of the target with a parabola (see Fig. 1) is to solve the following system:

$$\varphi_0 + \beta i + \alpha i^2 = \varphi_i \quad i \in [1, N_{sample}] \quad (1)$$

Where $(\varphi_0, \beta, \alpha)$ are the parabola coefficients and φ_i represent the phase samples, N_{sample} being the number of sample used to compute the azimuthal spectrum of the moving target. By inverting the system (1), we obtain the defocusing measurement accuracy (noted σ_α):

$$\sigma_\alpha \propto \frac{1}{N_{ech}^2 \sqrt{SCR}}$$

As $\alpha \propto \frac{1}{N_{ech}^2}$ [4], we can show that the azimuth velocity and radial acceleration measurement accuracy (given by the defocusing measurement accuracy σ_α) depends on the SCR of the target:

$$\sigma_{m_v} \propto \frac{1}{\sqrt{SCR}}$$

The delocalization of a moving target in azimuth induces a phase slope. The inversion of the system (1) gives us the measurement accuracy of this slope, noted σ_β :

$$\sigma_\beta \propto \frac{1}{N_{ech} \sqrt{SCR}}$$

The shift theorem for Fourier transform gives us:

$$\sigma_i \propto \frac{1}{\sqrt{SCR}}$$

For example, we consider a moving target ($P_{signal,dB} = 10dB$) in urban context ($\sigma_0 \cong -10dBm^2.m^{-2}$ given by [6]).With the point-like scatterers approach, we obtain subpixellic measurement accuracy ($\sigma_i < 0.1pixel$), thanks to the moving target signal analysis.

3.2 Measurement accuracy extended targets model:

The second approach is to consider extended targets, that is, targets with a physical surface. This approach is closer to real cases. In this case we are limited by the azimuth resolution and by the radiometric properties of the moving targets. Indeed, the azimuth resolution ρ_{az} is linked to the integration time T_{int} by:

$$\rho_{az} \cong 0.88 \frac{\lambda D}{2T_{int} V_P}$$

Extended moving targets can be modeled by a finite number of bright spots, and the distribution of these spots is random, and depends both on the target and view angle. Therefore, when ρ_{az} increases, T_{int} increases and the probability that the distribution changes during the integration time will increase. So in this case, the target position estimation accuracy is in the range of the target dimension (that is to say metric errors in the case of targets in urban context).

4. Estimation of the covariance matrix of the output parameters

All the measurement accuracies lead us to a covariance matrix, noted Γ_Y . In our methodology, an optimal moving target trajectory reconstruction calls for a minimisation of the system error function. This function is given by:

$$\Phi(\mathbf{X}, \mathbf{Y}) = \sum_{i=1}^{3*N} f_i^2(\mathbf{X}, \mathbf{Y})$$

Where f_i are the equations used for our system solving (see [4]), and N the number of images used. \mathbf{X} represents the output parameters and \mathbf{Y} the measurements. By non-linear least squares inversion, we obtain an expression of the covariance matrix of the output parameters:

$$cov(\tilde{\mathbf{X}}) = \nabla f(\mathbf{Y})^T \Gamma_Y \nabla f(\mathbf{Y})$$

Where $\nabla f(\mathbf{Y})^T$ is a combination of Jacobian, Hessian and other partial derivatives matrix calculated for the solution of the system, noted \mathbf{X}^* . Therefore, $cov(\tilde{\mathbf{X}})$ depends on the measurement accuracies and thus on moving target models. Fig. 2 shows an example of the estimated position accuracy (given by $cov(\tilde{\mathbf{X}})$) of a target trajectory with constant velocity, for a perfect synthetic aircraft circular trajectory and different configurations. The x axis represents the number of images N_{images} used to invert the problem, the y axis represents the total angle used – that is $N_{images} * \theta$, with θ the integration angle of a single image. We generate independent data, in order to study the impact of N_{images} and of the image resolution.

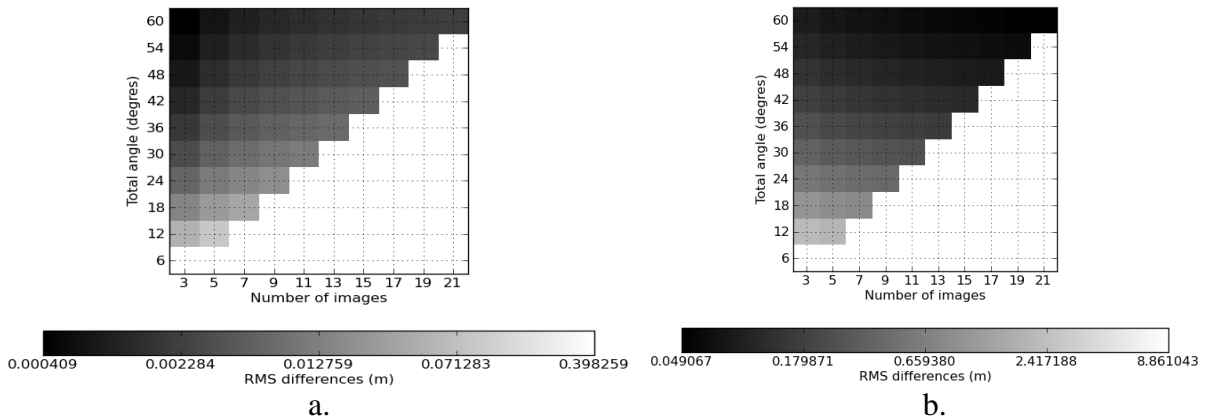


Fig. 2: RMS differences for a trajectory with constant velocity (10m/s toward North-East direction). a.: case of targets as point-like scatterers. b.: case of extended anisotropic scatterers.

Therefore, for a given total angle (y axis), the fewer images we have, the better resolution we get, because of the increase of θ . Obviously the results improved with the total angle, and we obtain better results with the point-like approach (the average error is about 1.5cm) than with the extended anisotropic approach (the average error is about 45cm). These results also show

that for a given angle, a small set of images with a good resolution gives better results than a large set of images with a lower resolution in the case of point-like scatterers. The opposite is reported in the case of extended targets: a large set of images, even with a lower resolution, gives us better results than a small set with a good resolution. We can suppose that in real cases, because each backscatterer can be considered as a bright point over a small integration angle, we will observe a combination of these two behaviours.

5. Experimental results analysis

Images are acquired with the SETHI sensor from ONERA which is described in [4]. The data are X-band data with decimetric slant range resolution, and we examine a moving target which is supposed to be a train: we see several horizontal lines like as if it were due to train wagons (see Fig. 3). The curvature of the horizontal lines is due to range migration, which appears on images with high azimuth resolution.

The simplest way to refocus the moving target is to compute the azimuthal spectrum of the moving target and to fit a parabola to its phase behavior. Because of the extended anisotropic behavior of the moving targets, their phase histories are in most cases a complex sum of parabola. To choose the best phase correction, we select a patch containing the moving target (see Fig. 3) and we maximize in the image domain a sharpness ratio [1][5] applied to the patch. The ratio is given by:

$$C = \frac{\sum_{x,y} |g_{cor}(x,y)|^4}{\sum_{x,y} |g(x,y)|^4}$$

Where $g(x,y)$ represents the complex image in the patch before phase correction and $g_{cor}(x,y)$ represents the complex image in the patch after correction. In most cases in urban context, we obtain two main peaks: one corresponding to the clutter focusing and one for the moving target focusing. If the SAR images are well focused for still targets, the amplitude of the sharpness peak corresponding to the clutter focusing is equal to 1, and the amplitude of the moving target peak is different from 1. A simple test on the value of the peak leads us to the selection of the right phase correction (see Fig. 3). This method was tested on the Nimes dataset. A result is presented in Fig3. The target is 100m long. This length corresponds to the length of a TER (Train Express Regional), and such a train often travels in Nimes.

Then we apply our inversion algorithm to obtain the real trajectory of the train. We took an angle between the two farthest images equal to 18° (10 images). The measured velocity of the moving target is almost constant and equal to $10m/s$ ($37km/h$). The result of the trajectory computation is shown in the green circle. All these characteristics are consistent with a train arrival in the Nimes station (red circle). A work on a set of real known trajectories will enable us to confirm this good result.

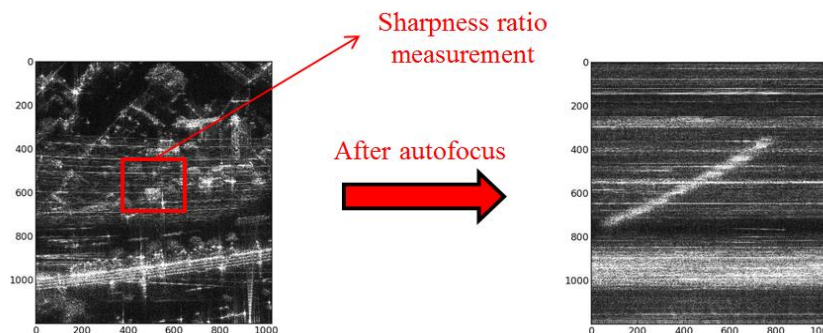


Fig. 3: an example of a signature of a moving target on a SAR image at the city of Nîmes (zoom). The azimuth direction is horizontal so the defocusing effect appears as horizontal lines.

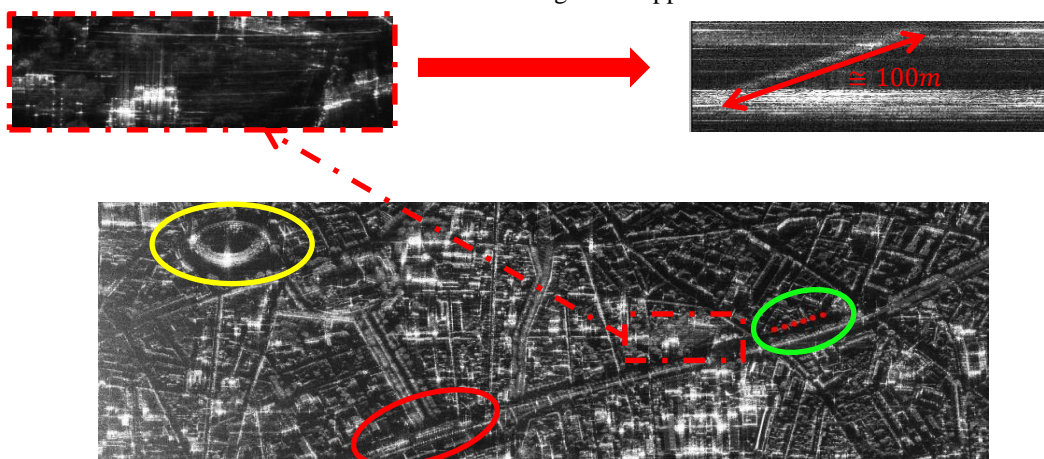


Fig. 4: trajectory reconstruction for a real unknown trajectory. Red circle is the train station of the city of Nîmes (Nîmes arena is in the yellow circle)

5. Conclusion

In this paper, we presented a performance analysis of a method for tracking moving targets using airborne SAR images acquired on a circular trajectory. This method is divided into two main steps: an autofocus algorithm and a tracking algorithm. Two different moving target hypotheses were presented and the results on measurements accuracy and estimated position accuracy have shown the potentiality of the method and the impact of several parameters (difference of heading angles, number of measurements) on the trajectory reconstruction accuracy. The new result on real data confirms these theoretical considerations. A work on a set of real known trajectories will enable us to definitively quantify the performance of the method on real cases.

References:

- [1] J. Fienup, "Detecting moving targets in SAR imagery by focusing", IEEE Transactions on Aerospace and Electronic Systems, 32 (July 2001), 794-808.
- [2] R. Raney, "Synthetic aperture imaging radar and moving targets". IEEE Transactions on Aerospace and Electronic Systems, 7, 3 (1971), 499-505.
- [3] P. Marques, J.Dias, "Velocity estimation of fast moving targets using a single SAR sensor", IEEE transaction on Aerospace and Electronic Systems, 41,1 (2005) 75-89.
- [4] J.B. Poisson, H. Oriot, F. Tupin, "Moving Target tracking using circular SAR imagery", EUSAR'12, Nuremberg, Germany, 2012.
- [5] F. Berizzi, G. Corsini, "Autofocusing of inverse synthetic aperture radar images using contrast optimization", IEEE Transactions on Aerospace and Electronic Systems, 32 (1996), 1185-1191.
- [6] F.T. Ulaby, M.C. Dobson, "Handbook of Radar Scattering Statistics for Terrain", Artech House, Inc., Dedham, Massachusetts, 1989, 362 pages.
- [7] W.Ye, T.S.Yeo, Z. Bao, "Weighted Least-Squares Estimation of Phase Errors for SAR/ISAR Autofocus", IEEE Transactions on Geoscience and Remote Sensing, 37, 5 (1999), 2487-2494.